Published in final edited form as:
Biomaterials. 2009 December ; 30(34): 6593–6603. doi:10.1016/j.biomaterials.2009.08.031.

Characterization of Valvular Interstitial Cell Function in Three Dimensional Matrix Metalloproteinase Degradable PEG Hydrogels

Julie A. Benton[a], **Benjamin D. Fairbanks**[a], and **Kristi S. Anseth**[a,b,*]

[a]Department of Chemical and Biological Engineering, University of Colorado, Boulder, CO, 80309-0424, USA

[b]Howard Hughes Medical Institute, University of Colorado, Boulder, CO, 80309-0424, USA

Abstract

Valvular interstitial cells (VICs) maintain functional heart valve structure and display transient fibroblast and myofibroblast properties. Most cell characterization studies have been performed on plastic dishes; while insightful, these systems are limited. Thus, a matrix metalloproteinase (MMP) degradable poly(ethylene glycol) (PEG) hydrogel system is proposed in this communication as a useful tool for characterizing VIC function in 3D. When encapsulated, VICs attained spread morphology, and proliferated and migrated as shown through real-time cell microscopy. Additionally, fibronectin derived pendant RGD was incorporated into the system to promote integrin binding. As RGD concentration increased from 0 to 2000 μM, VIC process extension and integrin$\alpha_v\beta_3$ binding increased within two days. By day 10, integrin binding was equalized between conditions. VIC morphology and rate of process extension were also increased through decreasing the hydrogel matrix density presented to the cells. VIC differentiation in response to exogenously delivered transforming growth factor-beta1 (TGF-β1) was also examined within the hydrogel networks. TGF-β1 increased expression of alpha smooth muscle actin (αSMA) and collagen-1 at both the mRNA and protein level by day 2 of culture, indicating myofibroblast differentiation, and was sustained over the course of the study (2 weeks). These studies demonstrate the utility, flexibility, and biological activity of this MMP-degradable system for the characterization of VICs, an important cell population for tissue engineering viable valve replacements and understanding valvular pathobiology.

Keywords

Fibroblast; Heart valve; Hydrogel; Peptide; Photopolymerisation; Matrix metalloproteinase

1. Introduction

Valvular interstitial cells (VICs) are the main cell population of the cardiac leaflets. When these cells are isolated from fresh tissue and plated on traditional two-dimensional plastic dishes, they undergo a wound-healing response and begin to differentiate from quiescent fibroblasts

*Corresponding Author: University of Colorado Campus Box 424 Boulder, CO, 80309-0424, USA Phone: (303) 492-3147 Fax: (303) 735-0095 kristi.anseth@colorado.edu.

to activated myofibroblasts, giving rise to a heterogeneous population [1,2]. Furthermore, VIC monolayer contractility leads to the formation of multicellular aggregates and calcified nodule structures on traditional culture surfaces [3–5]. Hence, a culture system that would allow VIC characterization under conditions more reminiscent of native valve properties is highly desirable. Polymeric 3D hydrogel materials based on a variety of chemistries have been introduced for this purpose [6–8]. Development of appropriate 3D culture scaffolds for VIC characterization is exceedingly important for tissue engineers to generate viable valve replacements, in addition to providing tools for studying VIC biology and pathology in efforts to better treat valvular disease.

In past studies, VICs have been cultured primarily in 3D matrices derived from natural materials. The most widely studied being collagen followed by fibrin-based materials [7,9, 10]. Although these materials provide 3D scaffolds that support cell viability, their material properties are difficult to control and cannot be loaded under physiologically relevant conditions. Furthermore, due to the contractile and remodeling activity of VICs, collagen matrices are quickly compacted by the cells to at least half their original size [4,10,11]. Beyond material properties, protein matrices interact with cells in a complex manner by coupling membrane receptors and initiating signaling cascades that direct cell differentiation, proliferation, and migration [7,12,13]. Natural proteinaceous materials also serve as a reservoir for bioactive molecules by sequestering growth factors and cytokines from the media [14–16]. These intricate biological interactions make it exceedingly difficult to deconvolute the effects of specific material interactions on VIC functions. To address these challenges, we investigated a newly developed bioactive synthetic hydrogel [17] for 3D VIC culture.

This hydrogel system consists of four-arm poly(ethylene glycol) (PEG) chains connected with enzymatically degradable peptides. PEG is a versatile synthetic polymer utilized extensively for 3D encapsulation due to its bioinert nature. Moreover, PEG can be easily functionalized with numerous reactive groups to allow cytocompatible encapsulation with light irradiation [18–20]. Here, PEG was functionalized with norbornene reactive groups to allow radical photopolymerization with thiol functional groups on cysteine containing peptides. In this mechanism, gels form by radical mediated, one-to-one addition, leading to a regular polymer network structure [17]. In these gels, a matrix metalloproteinase (MMP) degradable peptide (GPQGIWGQ) was chosen to crosslink PEG chains to allow cell-dictated gel remodeling, as VICs are known to secrete a wide range of these enzymes [21–23]. This peptide sequence is derived from collagen motifs [24,25] and has been utilized previously in fabrication of degradable networks [8,26]. Finally, this system allows incorporation of additional peptides, such as those based on adhesion proteins (e.g., RGD) to tune integrin binding [27]. Here, we explore these novel MMP-degradable PEG hydrogels functionalized with RGD as a potential platform to study 3D VIC morphology, differentiation, proliferation, and migration.

2. Materials and methods

2.1 Hydrogel and peptide preparation

Four arm, poly(ethylene glycol) (PEG) (20,000 $\bar{M}_n$) (JenKemUSA) was functionalized with norbornene functional groups by addition of norbornene acid by symmetric anhydride N,N'-dicyclohexylcarbodiimide (DCC) coupling as previously described [17]. Briefly, 4-arm PEG was dissolved in dichloromethane (DCM) with pyridine and 4-(dimethylamino)pyridine (DMAP) (Sigma). In a separate vessel, DCC was reacted at room temperature with 5-norbornene-2-carboxylic acid anhydride. After stirring for 30 minutes, the PEG solution was added and stirred overnight. The mixture was then filtered, washed with sodium bicarbonate, and precipitated in ice-cold diethyl ether. Substitution and purity of the PEG-norbornene

product was determined to be > 95% as characterized by ^{1}H NMR with particular attention paid to the alkene proton peaks occurring between 6.3 and 5.9 ppm

The MMP degradable peptide and adhesive RGD peptide were synthesized on solid Rink-amide resin using Fmoc chemistry on a model 433A peptide synthesizer from Applied Biosystems or a Tribute peptide synthesizer from Protein Technologies. Lysines were added to the peptides to enhance solubility. All peptides were analyzed by reverse phase high-pressure liquid chromatography (HPLC) and MALDI mass spectroscopy. When purity was less than 95%, peptides were purified with HPLC. All peptides were lyophilized from water or water/acetonitrile solution. As peptides prepared by this method often contain substantial amounts of bound water, true peptide content was determined by using the absorbance of the peptide solution at 280 nm with a molar extinction coefficient for tryptophan of 5500 $M^{-1}cm^{-1}$. To verify the absorbance results and to verify the presence and content of reduced thiols, Ellman's assay (Pierce) was performed using a cysteine standard. The resulting PEG-norbornene and peptide sequences are given in Fig. 1.

2.2 Cell culture and encapsulation

VICs were isolated from surgically removed aortic cardiac leaflets from porcine hearts (Hormel) received within 24 hours after sacrifice by sequential collagenase digestion as previously described [28]. Cells were cultured in growth media (Medium 199, 15% fetal bovine serum (FBS), 2% penicillin/streptomycin (100 U/mL), 0.4% fungizone (0.5 μg/mL)) and successively passaged with trypsin digestion. All experiments utilized VICs at the second or third passage and were performed in low serum (1% FBS supplemented) media to minimize cell proliferation except where noted. Hydrogel VIC cultures were supplemented with TGF-β1 at 5 ng/mL where indicated.

VICs were suspended in stoichiometrically balanced monomer solutions (i.e. equal thiol to ene ratio) comprised of either 5 or 10 wt.% PEG-norbornene and MMP degradable peptide, 0.05 wt.% Igracure 2959 (photoinitiator), and 1000 μM CRGD adhesive peptide unless otherwise specified, in phosphate buffered saline (PBS) at a density of 15 million VICs / mL monomer solution. The cell-gel solution was injected between glass slides separated by a 1 mm spacer in circular molds (7 mm diameter), and exposed to UV light centered at 352 nm at 5 mW/cm^2 for 10 minutes to allow complete polymerization. The resulting cell-gel polymer discs were then transferred to cell media with indicated supplements and cultured for up to 21 days in a humid incubator at 37°C and 5% CO_2.

2.3 Live/dead staining and morphology analysis

VIC viability and morphology within the MMP-degradable PEG hydrogels were determined by live/dead staining (Invitrogen). Briefly, hydrogels were rinsed with PBS, and placed in phenol red-free media containing the live/dead stain for 30 minutes. VIC containing MMP-degradable PEG hydrogels were then rinsed and imaged utilizing confocal microscopy (LSM 5 Pascal, Achroplan 10x NA 0.3W, Carl Zeiss, Inc). For each gel, three image z-stacks 200 μm (10 μm slices) in height were taken and projected for image analysis. Cell area and circularity (circularity = 4π(area/perimeter^2)) were determined from projections of the live/dead image stacks using NIH ImageJ software analyze particles feature.

2.4 Immunostaining

Hydrogel constructs were fixed with 10% buffered formalin overnight at 4°C, then transferred to a 30 wt.% sucrose solution in PBS for an additional 24 hours at 4°C. Samples were then mounted in cryostat mounting medium, frozen, sectioned into 30 μm slices, and mounted on glass slides for immunostaining. Slides were rinsed and permeabilized in 0.05 wt.% Tween 20-supplemented PBS. Non-specific antibody staining was blocked with 3 wt.% bovine serum

albumin (BSA) containing PBS. Slides were then incubated with the specified primary antibodies (mouse anti-αSMA (Abcam), mouse anti-collagen 1 (Abcam), or mouse anti-integrin $\alpha_v\beta_3$ (Abcam)), at previously determined dilutions in 1 wt.% BSA containing PBS. Following primary antibody coupling, samples were washed and incubated with mouse-anti-goat alexa 488 (Invitrogen) and phalloidin-tetramethylrhodamine B isothiocyanate (Sigma-Aldrich). Slides were subsequently mounted with DAPI and imaged on a Nikon TE 2000 epifluorescence microscope. Images from each fluorescent channel were merged, and background flattened using MetaMorph (Molecular Devices). The number of cells was counted using the DAPI channel and ImageJ (NIH). Myofibroblasts and integrin positive cells were counted manually by identifying cells with positive staining, normalized to cell number from DAPI counts and expressed as a percentage.

2.5 mRNA isolation and quantifiable real-time polymerase chain reaction (qRT-PCR)

Messenger RNA (mRNA) was isolated from liquid nitrogen snap frozen VIC laden MMP-degradable PEG hydrogels using Trizol (Sigma-Aldrich). mRNA was then column purified with the Ambion RiboPure kit per manufacturer's instructions. Purity and amount of mRNA was confirmed with a NanoDrop spectrophotometer (Fisher). Reverse transcription was performed using the iScript cDNA Synthesis kit (Bio-Rad). Polymerase chain reaction (PCR) was then conducted using an iCycler qRT-PCR machine (Bio-Rad). Primers for GAPDH, α-SMA, and collagen-1 (Integrated DNA technologies) were previously reported [29]. Threshold cycle (C_T) and primer efficiency were analyzed according to the Pfaffl method and normalized to GAPDH [30].

2.6 Real-time cell tracking

Time lapse images of cell morphology and movement were captured in 400 μm z-stacks (15 μm slices) every 30 min over a 5 day period using a Nikon TE 2000 PFS fluorescent microscope equipped with a motorized stage and environmental sample chamber. Images were collected and analyzed using MetaMorph (Molecular Devices). Cell velocity was calculated from the average x and y displacements divided by the interval time between images (30 minutes).

2.7 dsDNA assay

Double stranded DNA (dsDNA) was isolated from similarly sized hydrogel constructs by papainase (Worthington) digestion at 60°C overnight. For each sample, two hydrogels were combined per digest sample. The resulting digestion solution was analyzed for dsDNA content using the Quant-It PicoGreen dsDNA assay (Invitrogen) per manufacturer's instructions.

2.8 Statistics

Data are presented as mean ± standard error of three or more samples. A ANOVA analysis was used to compare data sets, and the resulting *p* values that were used to determine statistical significance are indicated in figure captions.

3. Results

3.1 VIC proliferation in MMP-degradable PEG hydrogels

MMP-degradable PEG hydrogels form versatile ideal networks with tailorable bioactivity through peptide incorporation (Fig. 1). Within these constructs we investigated VIC proliferation, migration, and differentiation. VIC proliferative ability in response to serum induced growth conditions within MMP-degradable PEG hydrogels was studied. To visualize cell proliferation, VIC laden MMP-degradable PEG hydrogels were placed on a real-time cell tracking microscope in high serum (15% FBS) media. A filmstrip of recorded VIC division is

shown in Fig. 2A. In these images classic cell division is observed with the cell membrane contraction in the middle follow by separation of the daughter and parent cell.

Quantitatively, increased cell numbers were measured through analyzing gel dsDNA content over a two week time period. With high serum conditions (15% FBS), VIC dsDNA content increased in each hydrogel sample over low serum control (1% FBS) after 7 days of culture and continued over the time course of two weeks (Fig. 2B). A doubling of dsDNA was observed at day 7. In comparison, VIC doubling time in 2D cultures with high serum is on the order of hours and is contact limited [28].

3.2 VIC migration in MMP-degradable PEG hydrogels

In addition to proliferation, migration is an important cell process that requires a 3D matrix to capture critical aspects of the *in vivo* environment (e.g., a surrounding matrix that must be remodeled). Migration also plays a key role in VIC repair of valve tissue in response to injury [31]. To investigate VIC ability to migrate within MMP-degradable PEG hydrogels, VICs were encapsulated with 1000 μM pendant RGD and cultured on a real-time microscope in low serum (1% FBS) conditions to track cell movement. Images of 400 μm brightfield z-stacks were captured and projected every 30 minutes for three days. Cell paths and velocities were analyzed with MetaMorph software and plotted on x–y scales (Fig. 3).

Cell paths indicate random migration with distances up to 30 μm or ~3 cell lengths on a time scale of hours. Further confirming the random path, cell velocities (Table, Fig. 3) were calculated from the x–y paths and include 0 μm/min showing no directional persistence. This is most likely the result of a uniform encapsulation environment. Also, it was observed that cells with migratory ability first achieved spread morphology that was maintained during cell movement.

3.3 Hydrogel density influence on VIC morphology

Changing the crosslinking density of the PEG-peptide network (accomplished by adjusting the weight percent monomer at which polymerization was performed) significantly affects VIC morphology. Decreasing this property decreases the polymer density and the number of peptides (or crosslinks) that must be enzymatically cleaved to permit cell spreading and motility. When initial monomer concentrations were reduced from 10 wt.% to 5 wt.% with estimated crosslinking densities of ~2.3 ± 0.3 mM and ~1.0 ± 0.2 mm respectively (calculated from rubber elasticity theory [32,33]), encapsulated VICs were able to achieve a spread morphology on a faster timescale, and almost completely spread within 7 days rather than 14 days required for VICs encapsulated in the more highly crosslinked hydrogels (Fig. 4A and B).

From the live/dead morphology images, it can be seen that VIC spreading was increased in the lower crosslinking density hydrogels at a more rapid rate than the hydrogels formed with 10 wt.% monomer (Fig. 4A). Furthermore when this difference was quantified by circularity analysis using NIH ImageJ software, with 1 = perfect circle and 0 = straight line, VIC morphology was more spread (i.e., less circular) in the gels with an inherently lower crosslinking density. Initially, both gel compositions promoted similar VIC circularity (~0.75) that gradually decreased with time as the cells further extended. This trend was enhanced in the less dense gel structure and reduced to 0.26 ± 0.03, which is very similar to the circularity of VICs on plastic substrates 0.28 ± 0.05. These results indicate that the VICs are able to degrade and penetrate the matrix faster in less dense hydrogels.

3.4 VIC morphology and interaction with the cell adhesive peptide RGD

VICs were photoencapsulated in MMP-degradable PEG hydrogels with varying amounts of the fibronectin-based adhesion ligand RGD (0 μm, 100 μm, 500 μm, 1000 μm, and 2000 μm), to explore the effect of pendant adhesive ligand density on VIC morphology. Cell-laden gels were imaged by live/dead to visualize cell morphology. Representative confocal projections (equal 200 μm sized stacks) are depicted in Fig. 5A.

Visually, VIC morphology became more extended as RGD within the network increased, indicating enhanced cell attachment to the network. To quantify the visual results, NIH ImageJ software was used to analyze projected cell area (Fig. 5B) and circularity (Fig. 5C). Quantitatively, average projected cell area increased by at least two-fold from gels with 0 μm RGD to 2000 μm, while 100, 500, and 1000 μm RGD calculated cell areas remained between these values as expected (Fig. 5B). Similarly, circularity decreased (with 1 indicating a perfect circle, and 0 a straight line) as RGD concentration increased. VICs within 1000 and 2000 μm RGD containing networks had the least circular morphology (~0.4) (Fig. 5C). Lower concentrations of RGD, 100 and 500 μm, had more circularity initially but decreased with time (Fig. 5C). In comparison, VICs on traditional plastic substrates have a circularity of ~0.28 ± 0.05, whereas VICs encapsulated within MMP degradable PEG hydrogels at the highest concentration of RGD (2000 μm) had the lowest circularity around 0.40 ±0.03.

To investigate cell interaction with the RGD sequence, 30 μm slices of cell-laden MMP-degradable PEG-VIC hydrogels were immunostained for the integrin pair $\alpha_v\beta_3$, a known RGD binding membrane receptor complex. At day 2, as RGD incorporation increased within the network, positive staining for integrin $\alpha_v\beta_3$ was observed (Fig. 6A and B). The highest level studied (2000 μm RGD) was similar to the 1000 μm RGD gels with no significant increase in integrin staining (Fig. 6B). No positive integrin staining was observed in hydrogels that contained no RGD peptide. By day 10 however, all three conditions examined, 0, 1000, and 2000 μm RGD, had similar positive staining for $\alpha_v\beta_3$ (100% positive cells) (Fig. 6). This is most likely the result of binding with cell-secreted matrix proteins at this later time point.

3.5 VIC myofibroblast differentiation in response to exogenously delivered transforming growth factor-beta1

VICs are known to differentiate in 2D cultures to activated myofibroblast cells in response to various factors, the most notable being transforming growth factor-beta1 (TGF-β1) [11]. Furthermore, VICs are also known to differentiate in response to the modulus [34] or stiffness of their environment. Stiff substrates (such as traditional plastic dishes) promote myofibroblastic activity, and lower modulus or soft substrates (such as PEG hydrogel surfaces) promote fibroblast activity [34]. Since the MMP-degradable constructs examined here are inherently softer than traditional culture dishes, exogenous TGF-β1 was delivered to VIC-laden MMP-degradable PEG hydrogels at the standard concentration of 5 ng/mL used in 2D cultures to test if this process was altered within the 3D gels. To examine myofibroblast differentiation, two common markers were followed, α-smooth muscle actin (αSMA) and collagen-1 expression. Interestingly, in the absence of TGF-β1, αSMA expression initially decreased at day 2 and then continued to rise at a slow rate (Fig. 7A, B, and C). On the other hand, TGF-β1-treated gels had an increase in αSMA that was maintained throughout the course of the experiments (Fig. 7A, B, and C).

Positive immunostaining for αSMA stress fibers can be seen visually at the later time points (day 14) (Fig. 7A). Increased staining was also quantified with image analysis and revealed elevated αSMA positive staining in the TGF-β1 treated samples compared to untreated controls (Fig. 7B). A significant difference in αSMA gene expression was also observed with qRT-PCR analysis with roughly a doubling in αSMA mRNA levels with TGF-β1 treatment (Fig. 7C).

By comparison, TGF-β1 has also been found to induce a doubling of αSMA in 2D VIC cultures after 48 hours [11].

In addition to αSMA expression, collagen-1 expression was also studied through immunostaining and qRT-PCR analysis. Similarly to αSMA, TGF-β1 increased the expression of collagen-1 at both the gene and protein expression levels (Fig. 8A and B). Collagen-1 protein expression was markedly increased with treatment of TGF-β1 as can be seen in the immunostaining images (Fig. 8A). Interestingly, collagen-1 expression was mostly localized to the cell body indicating that it is not able to diffuse away from the pericellular region. This increase in expression was analyzed quantitatively with qRT-PCR analysis of collagen-1 gene expression (Fig. 8B). Collagen-1 mRNA expression was roughly doubled with TGF-β1 treatment while control samples maintained a relatively constant level of expression. Interestingly, there was a slight drop in collagen-1 expression at day 2 similar to αSMA expression. Together, increased expression of αSMA and collagen-1 with TGF-β1 delivery indicates myofibroblast differentiation in these 3D gels.

4. Discussion

A novel enzymatically degradable hydrogel system was evaluated as a potential 3D culture platform for studying VIC function. This system consists of four-arm synthetic PEG chains linked together by MMP-degradable peptide sequences. To enhance functionality, the cell adhesive peptide RGD was also included in this system. The results show that this system permits VIC motility, proliferation, and differentiation. Thus far, there are few studies evaluating VIC function in 3D systems, mostly a result of the lack of available appropriate scaffolds [9,35]. While traditional 2D culture systems are important tools for cell characterization, there are inherent limitations in the use of such platforms. The MMP-degradable PEG system eliminates cell polarization to a 2D surface and presents a uniform elastic matrix that can be tuned through modification of hydrogel composition, addition of bioactive peptides, and incorporation of soluble factors. Conceptually, this type of environment is an enhanced mimic of the *in vivo* valve environment over traditional plastic dishes. This MMP-degradable system is presented as an additional tool for the study of VIC biology to broaden the scope of cell characterization. The study of VIC function is important for understanding VIC cell biology, necessary information for those interested in regenerating heart valve tissue and understanding valvular pathobiology.

Proof of proliferative ability was given by observing and recording a cell division event with live cell imaging and by measurements of gel dsDNA content over time in response to serum induced growth conditions (Fig. 2). Although these results suggest that VICs are able to proliferate within the gel matrix, more definitive assays, such as BrdU incorporation, and more detailed studies of VIC proliferation within the gel are required to fully characterize VIC proliferation trends within the constructs. In comparison to plastic culture dishes, VICs proliferated at a slower rate in the hydrogel environment; VIC doubling time is on the order of hours on plastic and on the order of days in the MMP-degradable hydrogel [28]. Slowing of proliferation in 3D hydrogels may possibly result from the necessity to degrade and remodel the surrounding matrix, leading to a lag time before proliferation occurs. Despite the slower proliferation, gels can be quite useful for long term culture. Also, VIC proliferation is contact inhibited on plastic dishes; after the formation of confluent monolayers, VICs tend to aggregate and differentiate into calcified structures not yet observed in *in vitro* 3D constructs [5]. This process of VIC calcific nodule formation has been shown to be dependent on the αSMA expression [4]. In the 3D MMP-degradable systems however, proliferation is not restricted in surface area and contact inhibition was not observed, nor the formation of aggregate structures indicating proliferation may be altered in comparison to plastic dishes.

VIC motility was also observed within the MMP degradable PEG hydrogel constructs. The ability to migrate in response to injury is very important to ensure appropriate wound healing response from resident fibroblast and myofibroblast cells such as VICs [36]. Furthermore, in tissue environments signals and cues to elicit cell migration are three dimensional in nature along with cell response. The system presented here allows 3D cell response to signals not attainable in traditional culture systems. Qualitatively, it was observed during tracking that cells with migratory ability first achieved spread morphology before movement, indicating degradation of the network is required for motility. In these studies, VIC migration was permitted but lacked directional persistence. Directed migration may be achievable in this system by incorporation of chemoattractant gradients and requires further investigation. Importantly, this result shows these hydrogel platforms support VIC movement and may provide interesting platforms to study directed cell migration in response to chemoattractants or injury models.

Degradation of this network is through cleavage of the MMP degradable peptide listed in Fig. 1. This peptide is derived from collagen motifs and has been shown to be degradable by a host of MMP cell secreted enzymes most notably, MMP-1, MMP-2, MM-3, MMP-7, and MMP-9 [24,25,37]. This sequence has also been used in other enzymatically degradable hydrogels for the study of fibroblast 3D migration [8,37,38]. There is debate as to which MMPs are secreted by VICs, but there is general agreement that VICs can produce and activate MMP-1, MMP-2, MMP-3, MMP-9, and MMP-13 [22,23]. The profile of VIC MMP secretion most likely relies on a number of confounding factors including cell differentiation status (quiescent or myofibroblast), time in culture, and integrin binding. In depth characterization of VIC MMP secretion was not examined in this communication, as MMP production and regulation is a complex and transient system [39,40] and outside the scope of this study.

An important property of this hydrogel system is its versatility. Changing the amount of monomer used during polymerization alters the final hydrogel material properties. By altering gel composition, crosslinking density, and modulus, the density of the hydrogel matrix presented to the encapsulated cells changes. Furthermore, VICs, like other myofibroblast cells [41], are known to be responsive to matrix elasticity [34], which can be tuned in this system to elicit specific cell behaviors. Furthermore, rates of cell migration will also be influenced by network density [38]. In which case, migration may be tunable based on the network density. As shown, VICs indeed responded to changes in the density of the gel system (Fig. 4). When less dense gels were used, VICs achieved a spread morphology in 7 days rather than 14 days. As more monomer is incorporated during gelation, VIC morphological changes are slowed, as there is a larger barrier to process extension in the denser matrix.

To increase VIC biological interaction with the hydrogel network, bioactivity can be added to the system through the incorporation of additional peptides beyond the MMP-degradable structural linkages. Here, the cell adhesive peptide RGD was included. This peptide sequence has been widely used in 3D PEG based culture systems [42,43] and is primarily derived from the matrix protein fibronectin [27], though it can be found in numerous other proteins including the latent TGF-β1 binding complex [44]. Although RGD was used here, many other candidate sequences can easily be incorporated to alter cell adhesion to the network such as DGEA (from collagen-1) [45], IKVAV and YIGSR (both from laminin) [46,47]. Bioactivity of the network could also be altered by including peptides that sequester specific growth factors that activate myofibroblast VICs (e.g. WSHW binds active TGF-β1 [48]) [11], or by the addition of short peptide sequences that mimic growth factors that prevent VIC activation (e.g. F2A4-K-NS mimic of FGF-2 activity [49]) [50].

In this system, increasing the incorporation of RGD increased cell process extension (Fig. 5) producing more elongated cell morphologies. In addition, increased RGD content intensified

VIC expression of the integrin pair $\alpha_v\beta_3$, a known RGD binding integrin [27] at early time points. This result indicates that VICs are able to sense and respond to incorporated peptides. Interestingly, it has also been shown that this particular integrin pair can interact with MMPs and increase their activity [51–53]. This may also explain why more elongated cell morphologies are observed in MMP-degradable gels with large amounts of RGD incorporation. At later time points, $\alpha_v\beta_3$ integrin staining increased without RGD incorporation as well. By this point in culture, the VICs have most likely excreted matrix proteins including fibronectin in their pericellular space enhancing integrin activity independent of RGD [18]. It should also be noted, however, that increased incorporation of RGDS leads to a slightly lower crosslinking density within the hydrogels due to their pendant incorporation and may also influence the observed VIC morphology differences between conditions.

In addition to VIC migration and proliferation, differentiation was also studied in the MMP-degradable PEG hydrogel system in response to exogenously delivered TGF-β1, a potent fibrotic growth factor [11]. VIC transition from a fibroblast to myofibroblast phenotype is implicated in progression of valvular stenosis [4] and important to understanding valve biology and function. Here, when TGF-β1 was added to the system, αSMA and collagen-1 expression increased at both the mRNA and protein levels indicating myofibroblast differentiation (Fig. 7 and 8). This process has also been observed on traditional plastic substrates [11]. While we observed an increase in marker expression, we did not observe hydrogel contraction as is observed with VIC culture in collagen gels [9]. Rather all samples showed a degree of increased swelling with time in culture as the matrix was eroded. This may be due, in part, to the lack of fibrillar structure in our hydrogel samples; in collagen gels, VICs are able to generate force to align collagen fibers, here no such fibers exist. Interestingly, expression of both factors decreased initially and then gradually increased in the control conditions as well. VICs are known to be responsive to mechanical environments, where softer or lower moduli systems produce fibroblast-dominated populations and stiff systems increase myofibroblast differentiation [34]. This initial drop in myofibroblast differentiation may be a response to the mechanical change from stiff plastic to low modulus gel, but requires further investigation to fully explain this observation. Nonetheless, VICs were TGF-β1 responsive within a week in the MMP-degradable hydrogels suggesting that this system may be a useful tool for studied VIC differentiation in 3D.

5. Conclusions

We have demonstrated that VIC migration, proliferation, and differentiation are supported with MMP-degradable PEG hydrogels systems. These networks have a defined architecture that allows tuning of network density and ligand incorporation to control cell-material interactions, as well as the rate of cell process extension and matrix degradation. By combining biological and synthetic components, incredible flexibility and versatility can be achieved, making this system a useful tool for characterizing VIC biology. In addition to the peptide sequences studied here, many others could be incorporated to more precisely examine VIC-matrix interactions. Three-dimensional systems for characterizing VIC function and pathobiology are increasingly important for regenerating function valve tissue and understanding valvular disease evolution in a model more reminiscent of the native valve environment.

Supplementary Material

Refer to Web version on PubMed Central for supplementary material.

Acknowledgments

The authors thank Ms. Sarah M. Trexler, Ms. Nicole J. Darling, and Mr. Nicholas J. Alvey for experimental assistance. Input on manuscript preparation from Dr. Peter D. Mariner is also gratefully acknowledged. Dr. Sun's laboratory at NIAID is also gratefully acknowledged for supplying recombinant human TGF-β1. Funding for these studies was provided by NIH (HL089260) and HHMI. Funding for individual fellowships to JAB from NSF Graduate Research Fellowship Program (NSF GRFP) and Department of Education Graduate Assistantships in Areas of National Need (DoEd GAANN), and for BDF from DoEd GAANN are also gratefully acknowledged.

References

1. Filip DA, Radu A, Simionescu M. Interstitial-Cells of the Heart-Valves Possess Characteristics Similar to Smooth-Muscle Cells. Circulation Research 1986;59(3):310–320. [PubMed: 3769149]
2. Messier RH, Bass BL, Aly HM, Jones JL, Domkowski PW, Wallace RB, et al. Dual Structural and Functional Phenotypes of the Porcine Aortic-Valve Interstitial Population - Characteristics of the Leaflet Myofibroblast. Journal of Surgical Research 1994;57(1):1–21. [PubMed: 8041124]
3. Benton JA, Kern HB, Anseth KS. Substrate Properties Influence Calcification in Valvular Interstitial Cell Culture. Journal Of Heart Valve Disease 2008;17(6):689–699. [PubMed: 19137803]
4. Benton JA, Kern HB, Leinwand LA, Mariner PD, Anseth KS. Statins block calcific nodule formation of valvular interstitial cells by inhibiting alpha-smooth muscle actin expression. Arterioscler Thromb Vasc Biol. 2009Accepted
5. Mohler ER, Chawla MK, Chang AW, Vyavahare N, Levy RJ, Graham L, et al. Identification and characterization of calcifying valve cells from human and canine aortic valves. Journal Of Heart Valve Disease 1999;8(3):254–260. [PubMed: 10399657]
6. Abbott A. Cell culture: Biology's new dimension. Nature 2003;424(6951):870–872. [PubMed: 12931155]
7. Grinnell F. Fibroblast biology in three-dimensional collagen matrices. Trends In Cell Biology 2003;13 (5):264–269. [PubMed: 12742170]
8. Raeber GP, Lutolf MP, Hubbell JA. Molecularly engineered PEG hydrogels: A novel model system for proteolytically mediated cell migration. Biophysical Journal 2005;89(2):1374–1388. [PubMed: 15923238]
9. Taylor PM, Allen SP, Dreger SA, Yacoub MH. Human cardiac valve interstitial cells in collagen sponge: A biological three-dimensional matrix for tissue engineering. Journal of Heart Valve Disease 2002;11(3):298–306. [PubMed: 12056719]
10. Montesano R, Orci L. Transforming Growth Factor-Beta Stimulates Collagen-Matrix Contraction By Fibroblasts - Implications For Wound-Healing. Proceedings Of The National Academy Of Sciences Of The United States Of America 1988;85(13):4894–4897. [PubMed: 3164478]
11. Walker GA, Masters KS, Shah DN, Anseth KS, Leinwand LA. Valvular myofibroblast activation by transforming growth factor-beta - Implications for pathological extracellular matrix remodeling in heart valve disease. Circulation Research 2004;95(3):253–260. [PubMed: 15217906]
12. Ehrlich HP, Allison GM, Leggett M. The myofibroblast, cadherin, alpha smooth muscle actin and the collagen effect. Cell Biochemistry and Function 2006;24(1):63–70. [PubMed: 15584087]
13. Watson KE, Parhami F, Shin V, Demer LL. Fibronectin and collagen I matrixes promote calcification of vascular cells in vitro, whereas collagen IV matrix is inhibitory. Arterioscler Thromb Vasc Biol 1998;18(12):1964–1971. [PubMed: 9848891]
14. Fava RA, McClure DB. Fibronectin-Associated Transforming Growth-Factor. Journal Of Cellular Physiology 1987;131(2):184–189. [PubMed: 3495542]
15. Jones JI, Gockerman A, Busby WH, Camachohubner C, Clemmons DR. Extracellular-Matrix Contains Insulin-Like Growth-Factor Binding Protein-5 - Potentiation Of The Effects Of Igf-I. J Cell Biol 1993;121(3):679–687. [PubMed: 7683690]
16. Somasundaram R, Ruehl M, Schaefer B, Schmid M, Ackermann R, Riecken EO, et al. Interstitial collagens I, III, and VI sequester and modulate the multifunctional cytokine oncostatin M. Journal Of Biological Chemistry 2002;277(5):3242–3246. [PubMed: 11711546]

17. Fairbanks BD, Schwartz MS, Halevi AE, Nuttelman CR, Bowman CN, Anseth KS. A versatile synthetic extracellular matrix mimic via thiol-ene photopolymerization. Advanced Materials. 2009Accepted
18. Salinas CN, Anseth KS. The influence of the RGD peptide motif and its contextual presentation in PEG gels on human mesenchymal stem cell viability. Journal Of Tissue Engineering And Regenerative Medicine 2008;2(5):296–304. [PubMed: 18512265]
19. Bryant SJ, Arthur JA, Anseth KS. Incorporation of tissue-specific molecules alters chondrocyte metabolism and gene expression in photocrosslinked hydrogels. Acta Biomater 2005;1(2):243–252. [PubMed: 16701801]
20. Weber LM, Anseth KS. Hydrogel encapsulation environments functionalized with extracellular matrix interactions increase islet insulin secretion. Matrix Biology 2008;27(8):667–673. [PubMed: 18773957]
21. Dreger SA, Taylor PM, Allen SP, Yacoub MH. Profile and localization of matrix metalloproteinases (MMPs) and their tissue inhibitors (TIMPs) in human heart valves. Journal of Heart Valve Disease 2002;11(6):875–880. [PubMed: 12479292]
22. Edep ME, Shirani J, Wolf P, Brown DL. Matrix metalloproteinase expression in nonrheumatic aortic stenosis. Cardiovascular Pathology 2000;9(5):281–286. [PubMed: 11064275]
23. Rabkin E, Aikawa M, Stone JR, Fukumoto Y, Libby P, Schoen FJ. Activated interstitial myofibroblasts express catabolic enzymes and mediate matrix remodeling in myxomatous heart valves. Circulation 2001;104(21):2525–2532. [PubMed: 11714645]
24. Fields R. Measurement Of Amino Groups In Proteins And Peptides. Biochemical Journal 1971;124 (3):581–&. [PubMed: 5135243]
25. Netzelarnett S, Fields G, Birkedalhansen H, Vanwart HE. Sequence Specificities Of Human Fibroblast And Neutrophil Collagenases. Journal Of Biological Chemistry 1991;266(11):6747–6755. [PubMed: 1849891]
26. West JL, Hubbell JA. Polymeric biomaterials with degradation sites for proteases involved in cell migration. Macromolecules 1999;32(1):241–244.
27. Ruoslahti E. RGD and other recognition sequences for integrins. Annu Rev Cell Dev Biol 1996;12:697–715. [PubMed: 8970741]
28. Johnson CM, Hanson MN, Helgeson SC. Porcine Cardiac Valvular Subendothelial Cells In Culture - Cell Isolation And Growth-Characteristics. Journal Of Molecular And Cellular Cardiology 1987;19 (12):1185–1193. [PubMed: 3327949]
29. Benton JA, DeForest CA, Vivekanandan V, Anseth KS. Photocrosslinking of gelatin macromers to synthesize porous hydrogels that promote valvular interstitial cell function. Tissue Engineering 2009;15In Press
30. Pfaffl MW. A new mathematical model for relative quantification in real-time RTPCR. Nucleic Acids Research 2001;29(9)
31. Hinz B. Formation and function of the myofibroblast during tissue repair. J Invest Dermatol 2007;127 (3):526–537. [PubMed: 17299435]
32. Anseth KS, Bowman CN, BrannonPeppas L. Mechanical properties of hydrogels and their experimental determination. Biomaterials 1996;17(17):1647–1657. [PubMed: 8866026]
33. Flory, P. Principles of Polymer Chemistry. Cornell University Press; Ithaca, NY: 1953.
34. Kloxin AM, Benton JA, Anseth KS. In situ elasticity modulation with dynamic substrates directs cell phenotype. Biomaterials. 2009Submitted
35. Shah DN, Recktenwall-Work SM, Anseth KS. The effect of bioactive hydrogels on the secretion of extracellular matrix molecules by valvular interstitial cells. Biomaterials 2008;29(13):2060–2072. [PubMed: 18237775]
36. Tomasek JJ, Gabbiani G, Hinz B, Chaponnier C, Brown RA. Myofibroblasts and mechano-regulation of connective tissue remodelling. Nat Rev Mol Cell Biol 2002;3(5):349–363. [PubMed: 11988769]
37. Raeber GP, Lutolf MP, Hubbell JA. Mechanisms of 3-D migration and matrix remodeling of fibroblasts within artificial ECMs. Acta Biomater 2007;3(5):615–629. [PubMed: 17572164]
38. Lutolf MP, Lauer-Fields JL, Schmoekel HG, Metters AT, Weber FE, Fields GB, et al. Synthetic matrix metalloproteinase-sensitive hydrogels for the conduction of tissue regeneration: Engineering

cell-invasion characteristics. Proceedings Of The National Academy Of Sciences Of The United States Of America 2003;100(9):5413–5418. [PubMed: 12686696]

39. Baker AH, Edwards DR, Murphy G. Metalloproteinase inhibitors: biological actions and therapeutic opportunities. Journal Of Cell Science 2002;115(19):3719–3727. [PubMed: 12235282]
40. Nabeshima K, Inoue T, Shimao Y, Sameshima T. Matrix metalloproteinases in tumor invasion: Role for cell migration. Pathol Int 2002;52(4):255–264. [PubMed: 12031080]
41. Hinz B, Mastrangelo D, Iselin CE, Chaponnier C, Gabbiani G. Mechanical tension controls granulation tissue contractile activity and myofibroblast differentiation. American Journal Of Pathology 2001;159(3):1009–1020. [PubMed: 11549593]
42. Hubbell JA. Bioactive biomaterials. Curr Opin Biotechnol 1999;10(2):123–129. [PubMed: 10209141]
43. Ruoslahti E, Pierschbacher MD. New Perspectives In Cell-Adhesion - Rgd And Integrins. Science 1987;238(4826):491–497. [PubMed: 2821619]
44. Wipff PJ, Rifkin DB, Meister JJ, Hinz B. Myofibroblast contraction activates latent TGF-beta 1 from the extracellular matrix. J Cell Biol 2007;179(6):1311–1323. [PubMed: 18086923]
45. Staatz WD, Fok KF, Zutter MM, Adams SP, Rodriguez BA, Santoro SA. Identification Of A Tetrapeptide Recognition Sequence For The Alpha-2-Beta-1-Integrin In Collagen. Journal Of Biological Chemistry 1991;266(12):7363–7367. [PubMed: 2019571]
46. Tashiro K, Sephel GC, Weeks B, Sasaki M, Martin GR, Kleinman HK, et al. A Synthetic Peptide Containing The Ikvav Sequence From The A-Chain Of Laminin Mediates Cell Attachment, Migration, And Neurite Outgrowth. Journal Of Biological Chemistry 1989;264(27):16174–16182. [PubMed: 2777785]
47. Iwamoto Y, Robey FA, Graf J, Sasaki M, Kleinman HK, Yamada Y, et al. Yigsr, A Synthetic Laminin Pentapeptide, Inhibits Experimental Metastasis Formation. Science 1987;238(4830):1132–1134. [PubMed: 2961059]
48. Young GD, Murphy-Ullrich JE. The tryptophan-rich motifs of the thrombospondin type 1 repeats bind VLAL motifs in the latent transforming growth factor-beta complex. Journal Of Biological Chemistry 2004;279(46):47633–47642. [PubMed: 15342643]
49. Lin X, Takahashi K, Campion SL, Liu Y, Gustavsen GG, Pena LA, et al. Synthetic peptide F2A4-K-NS mimics fibroblast growth factor-2 in vitro and is angiogenic in vivo. Int J Mol Med 2006;17(5):833–839. [PubMed: 16596268]
50. Cushing MC, Mariner PD, Liao JT, Sims EA, Anseth KS. Fibroblast growth factor represses Smad-mediated myofibroblast activation in aortic valvular interstitial cells. Faseb Journal 2008;22(6):1769–1777. [PubMed: 18218921]
51. Brooks PC, Stromblad S, Sanders LC, vonSchalscha TL, Aimes RT, StetlerStevenson WG, et al. Localization of matrix metalloproteinase MMP-2 to the surface of invasive cells by interaction with integrin alpha v beta 3. Cell 1996;85(5):683–693. [PubMed: 8646777]
52. Levinson H, Sil AK, Conwell JE, Hopper JE, Ehrlich HP. Alpha V integrin prolongs collagenase production through jun activation binding protein 1. Ann Plast Surg 2004;53(2):155–161. [PubMed: 15269586]
53. Silletti S, Kessler T, Goldberg J, Boger DL, Cheresh DA. Disruption of matrix metalloproteinase 2 binding to integrin alpha(v)beta(3) by an organic molecule inhibits angiogenesis and tumor growth in vivo. Proceedings Of The National Academy Of Sciences Of The United States Of America 2001;98(1):119–124. [PubMed: 11134507]

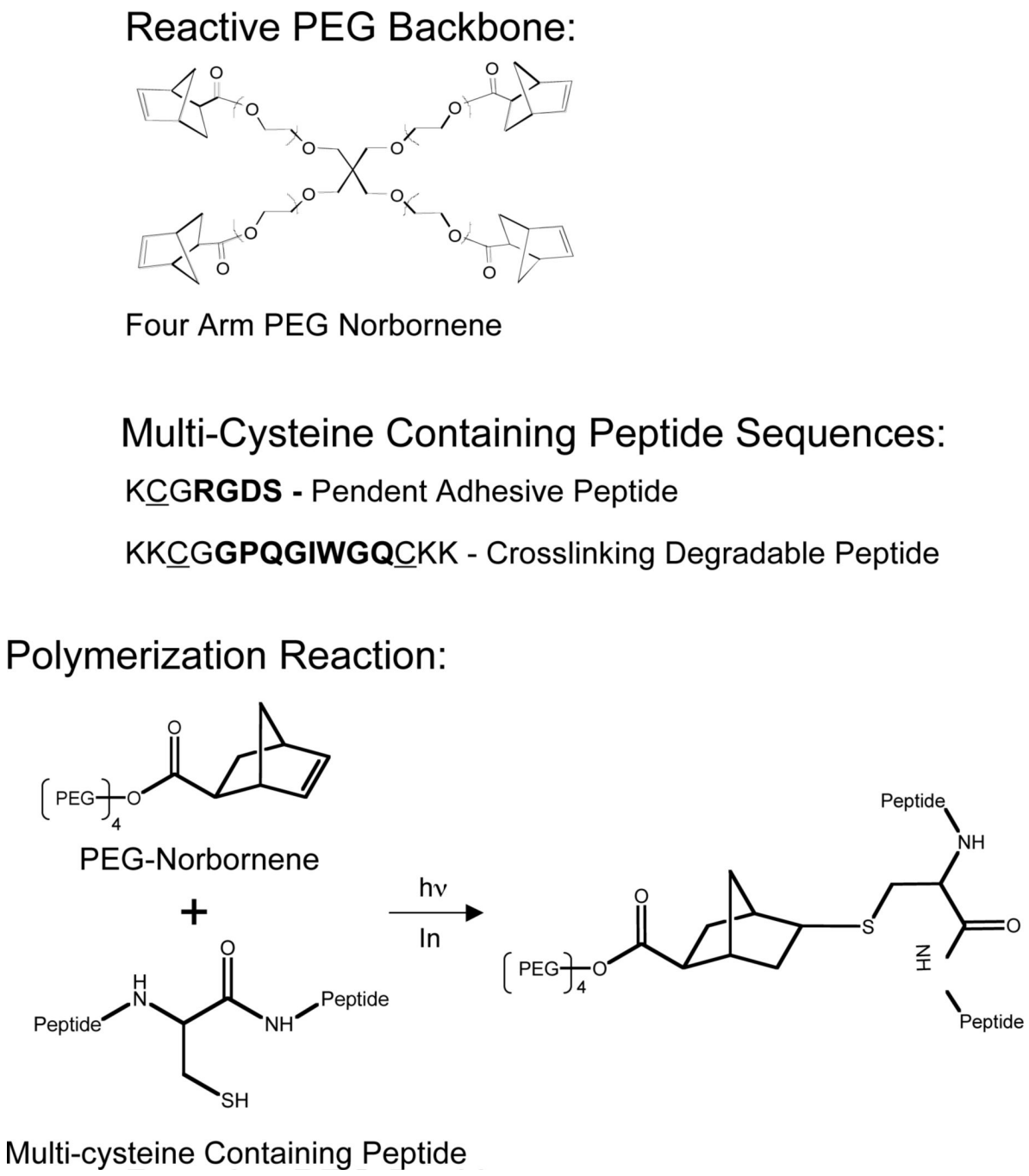

Fig. 1.
MMP-degradable PEG hydrogels were synthesized from the MMP-degradable peptide sequence and four-arm PEG-norbornene given. Networks form by alternating chain addition and chain transfer events leading to a step-growth-like regular network structure.

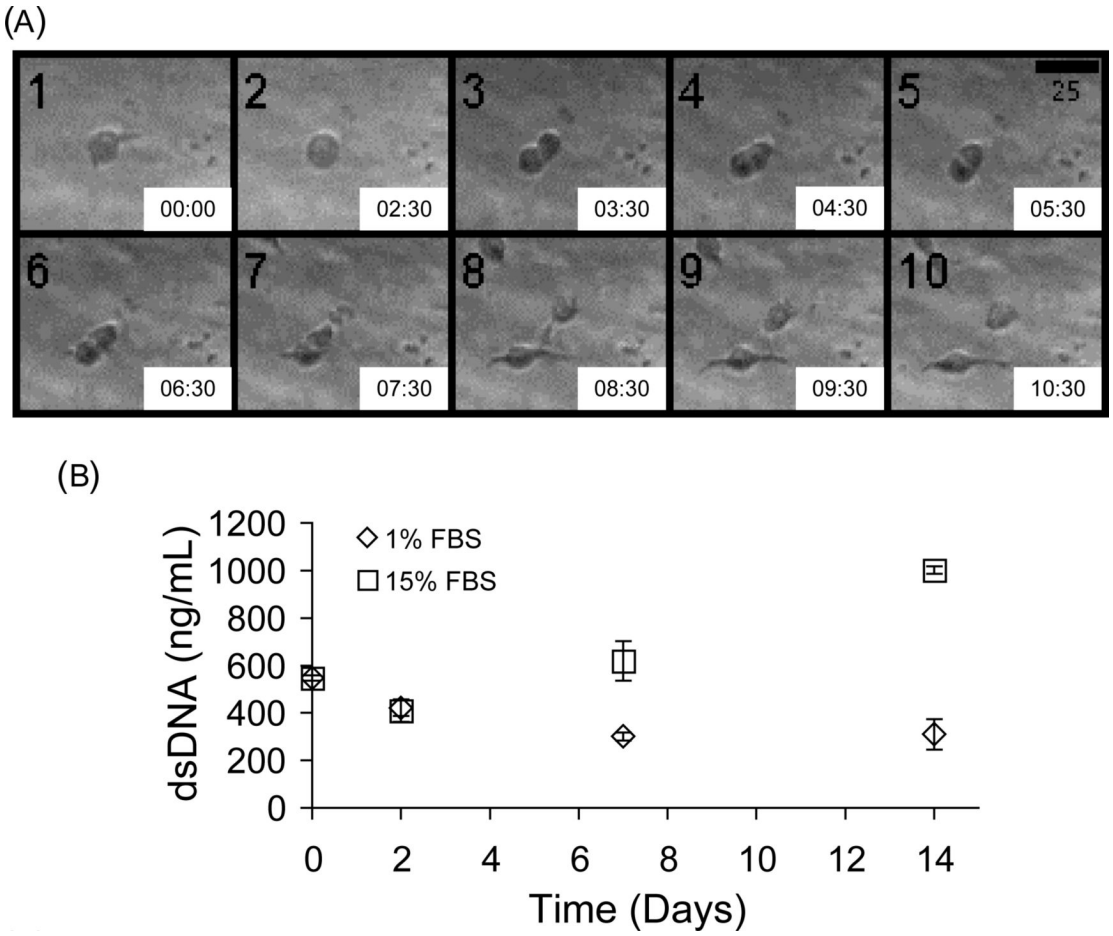

Fig. 2.

VICs were able to proliferate in response to high serum (15% FBS) within MMP-degradable PEG hydrogels (synthesized from 10 wt.% monomer formulations) containing 1000 μM pendant RGD. (A) Filmstrip of cell division event recorded with a real-time cell tracking microscopy. Time stamp presented as hours:minutes and scale bar indicates 25 μm. (B) dsDNA content of of digested VIC hydrogel solution (2 hydrogels per sample) cultured under the indicated serum conditions. n = 3.

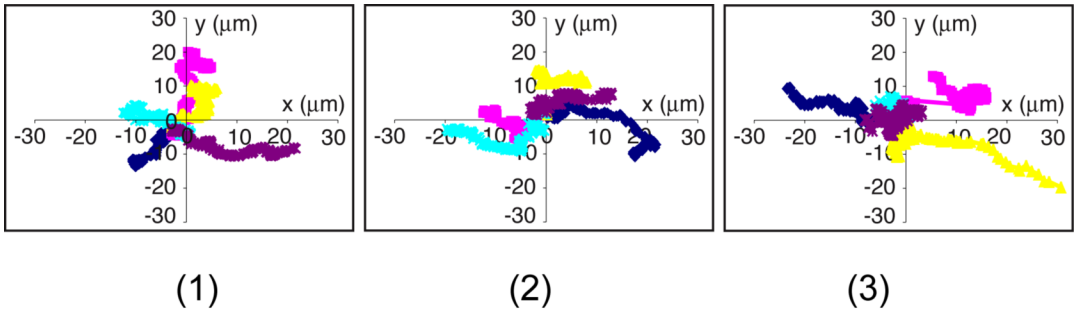

Position	Cell Velocity	
	x μm/min	y μm/min
1	-0.009 ± 0.04	0.02 ± 0.04
2	-0.02 ± 0.05	0.008 ± 0.03
3	-0.01 ± 0.02	0.0008 ± 0.02

Fig. 3.

VICs exhibited a random migration pattern within MMP-degradable PEG hydrogels (synthesized from 10 wt.% monomer formulations) containing 1000 μM pendant RGD under low serum conditions. Cells were imaged and tracked on a real-time microscope. Images of 400 μM brightfield z-stacks were captured every 30 minutes at different points in multiple hydrogels over a three day period and compressed to one plane with MetaMorph software. x–y plots represent five cell paths in three different gel positions over the time course of the experiment. Cell velocities were calculated from the x–y paths (n = 5) and include 0 μM/min.

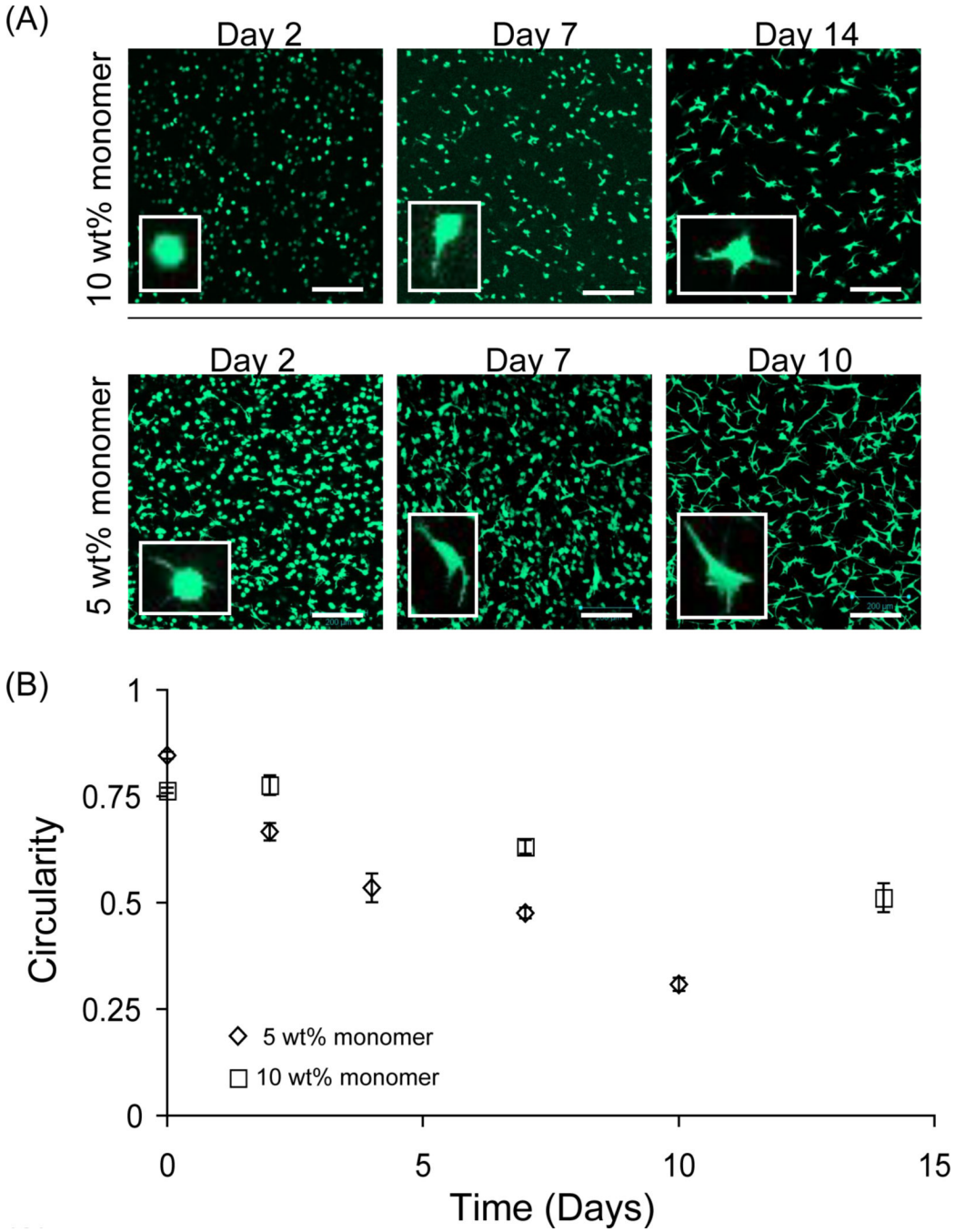

Fig. 4.

VIC process extension and spreading was more rapid in less dense μMP-degradable PEG hydrogel networks containing 1000 μM pendant RGD. (A) VIC laden μMP-degradable PEG hydrogels synthesized from 5 and 10 wt.% monomer solution were fabricated and imaged by live/dead staining with confocal microscopy. Presented images are 200 μM confocal z-stack projections where the scale bar indicates 200 μM. (B) Circularity was measured using NIH ImageJ software analyze particles function from the set of live/dead confocal images captured over the time course of the experiment. For each time point, three different hydrogels each had three pictures taken from various regions of the gel giving n = 3.

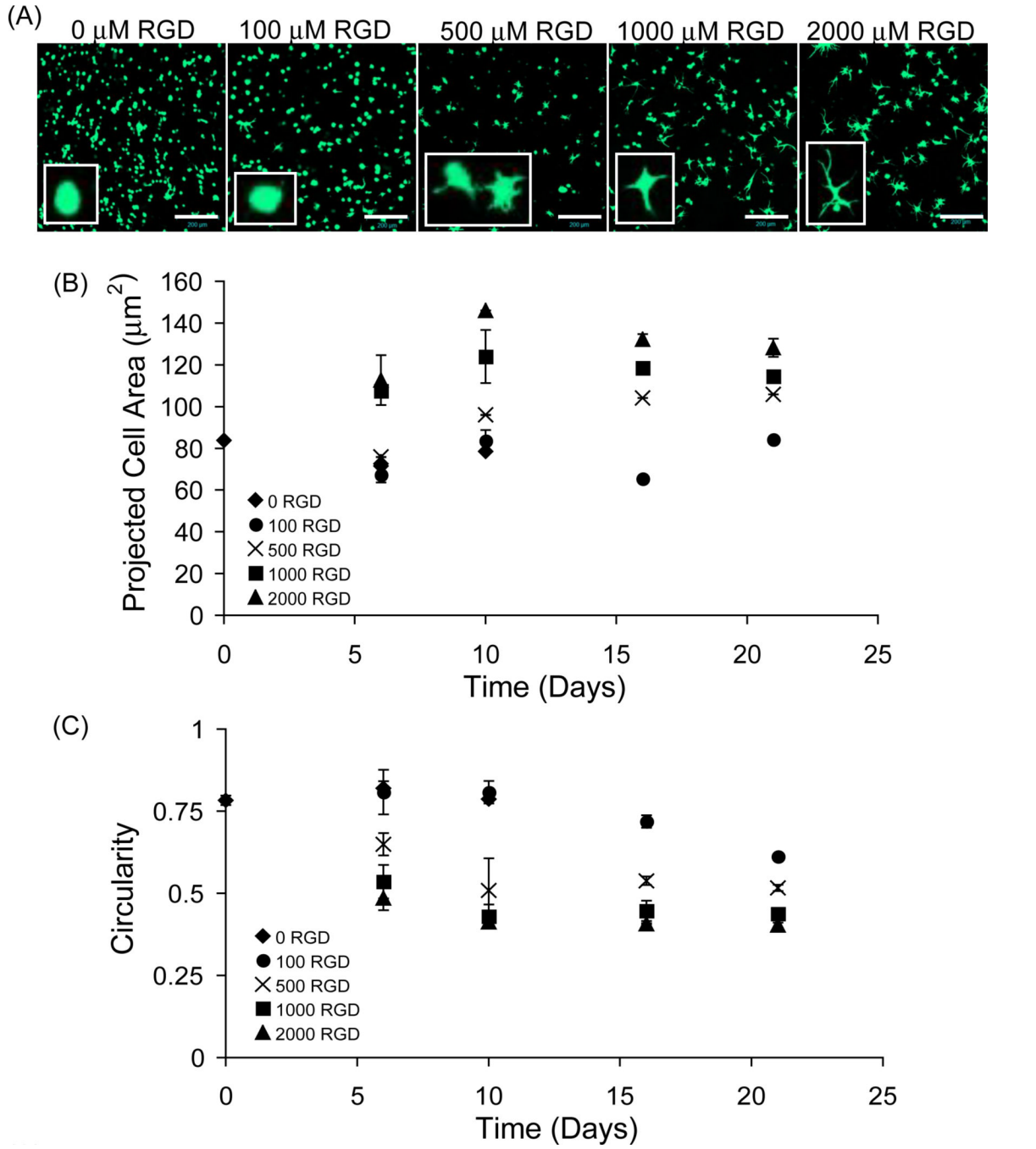

Fig. 5.

VIC morphology was influenced by varying pendant RGD peptide (0 – 2000 μM) incorporation within MMP-degradable PEG hydrogels (synthesized from 10 wt.% monomer formulations). (A) Representative live/dead stained confocal z-stack projections originally 200 μM in height. Images shown were captured 10 days after initial encapsulation with the indicated RGD concentrations. Scale bar indicates 200 μM. (B) Projected cell area was calculated from live/dead confocal stack projections using NIH ImageJ software analyze particles feature. Each time point and concentration had three pictures taken for 3 hydrogels for a total of nine pictures with n = 3 independent samples. Concentrations are given in μM. (C) Average circularity of cells was calculated by NIH ImageJ from the live/dead image set used for part (B).

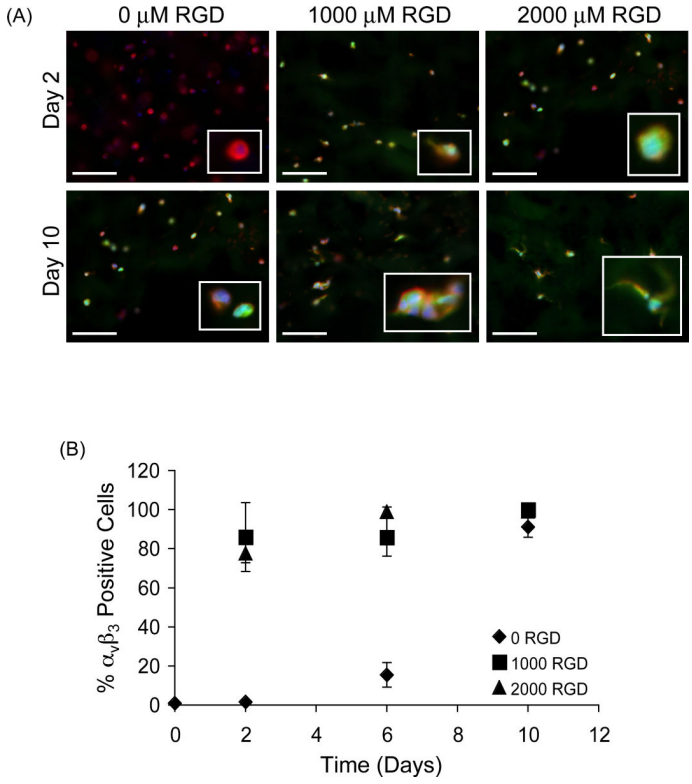

Fig. 6.

VICs interacted with the pendant RGD peptide within MMP-degradable PEG hydrogels (synthesized from 10 wt.% monomer formulations) through integrin pair $\alpha_v\beta_3$ binding interactions. (A) Representative immunostaining images for $\alpha_v\beta_3$ staining where green = $\alpha_v\beta_3$, red = F-actin, and blue = nuclei. Enlarged inlays are shown to highlight staining. Scale bar indicates 100 μM. (B) Image analysis of integrin pair $\alpha_v\beta_3$ immunostaining. Positive $\alpha_v\beta_3$ immunostaining was manually counted and normalized to total cell number from nuclei staining as counted by NIH ImageJ software. n = 5.

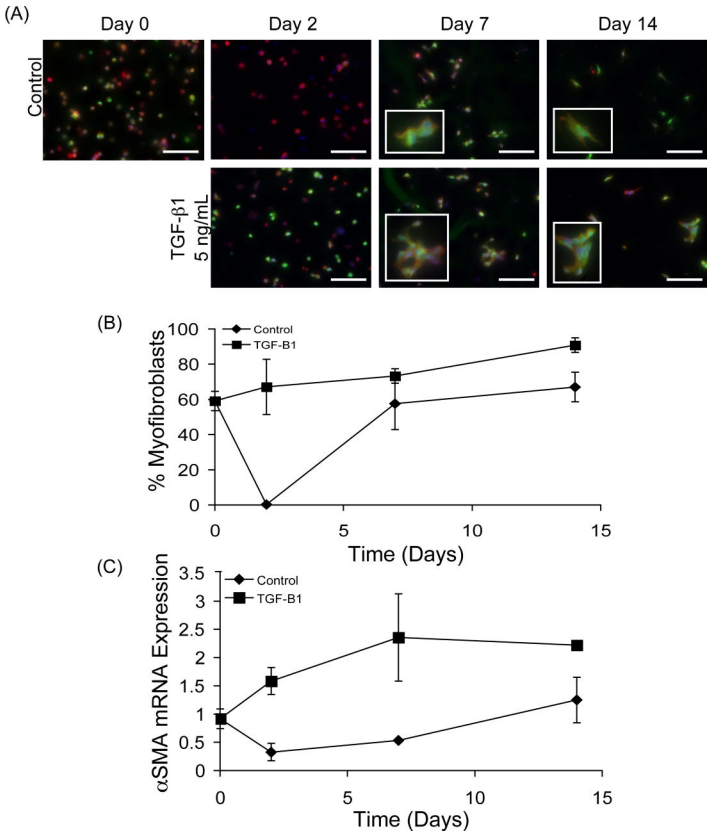

Fig. 7.

VICs encapsulated in μMP-degradable PEG hydrogels (synthesized from 10 wt.% monomer formulations) with 1000 μM pendant RGD incorporation expressed αSMA in response to exogenously delivered TGF-β1 (5 ng/mL). (A) Representative immunostaining images of αSMA stained hydrogel sections where green = αSMA, red = F-actin, and blue = nuclei. Inlay sections show enlarged cells to highlight αSMA presence. Scale bars indicate 100 μM. (B) Image analysis of immunostained sections. VICs were first counted from nuclei stains using NIH ImageJ analyze particles. Cells positive for αSMA were then manually counted and normalized to nuclei counts. n = 5. (C) GAPDH normalized qRT-PCR analysis of gene expression from control and TGF-β1 treated gels. Results have also been normalized to Day 0 control time point to show relative changes. n = 5.

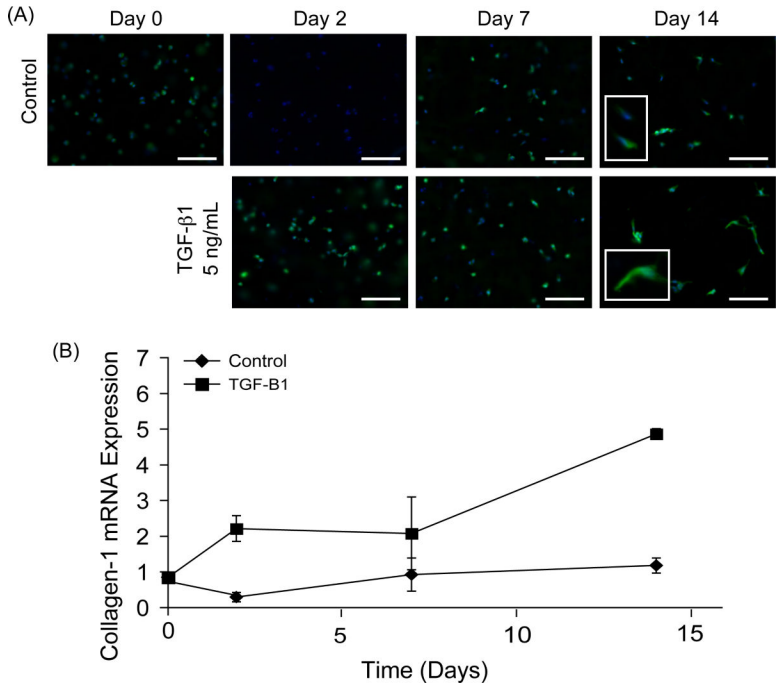

Fig. 8.

VICs encapsulated in MMP-degradable PEG hydrogels (synthesized from 10 wt.% monomer formulations) with 1000 μM pendant RGD expressed collagen-1 in response to exogenously delivered TGF-β1 (5 ng/mL). (A) Representative immunostaining images of helical collagen-1 stained hydrogel sections where green = collagen-1, and blue = cell nuclei. Inlay sections show enlarged cells to highlight helical collagen-1 presence. Scale bars indicate 100 μM. (B) GAPDH normalized qRT-PCR analysis of gene expression from control and TGF-β1 treated gels. Results have also been normalized to Day 0 control time point to show relative changes. n = 5.